Proceedings of the XVII ECSMGE-2019
Geotechnical Engineering foundation of the future
ISBN 978-9935-9436-1-3

doi: 10.32075/17ECSMGE-2019-0104

XVII European Conference
ECSMGE 2019
Reykjavik
on Soil Mechanics
and Geotechnical Engineering

Test results of friction resistance in the sleeper – ballast contact

Résultats d'essai de la résistance au frottement dans le contact couchette - ballast

M. Santana/ primary author
Laboratorio de Geotecnia/CEDEX/Madrid, Spain

J. Estaire
Laboratorio de Geotecnia/CEDEX/Madrid, Spain

ABSTRACT: This study evaluates the ballast-sleeper bottom shear friction from the testing of some specimens, performed in a very large direct shear box which has a shearing plane of 1x1 m and can hold specimens with a thickness up to 80 cm, so ballast can be tested using particles with their real dimensions.
The tests were performed by placing a half concrete sleeper at the shear plane box, once the bottom part of the shear box was filled with fresh and compacted ballast.
The results were compared with the previous results obtained for the ballast friction angle and for the friction between gravel and concrete elements. Furthermore, the results were also used to interpret some Single Tie Push Tests (STPT) performed in CEDEX Track Box to evaluate the track lateral resistance.

RÉSUMÉ: L´étude évalue le frottement entre ballast et traverse à partir de l´essai de certains spécimens effectué dans une très grande boîte de cisaillement direct qui présente un plan de cisaillement de 1x1 m et peut contenir des échantillons d'une épaisseur allant jusqu'à 80 cm, en utilisant des particules avec leurs dimensions réelles.
Les essais ont été effectués en plaçant une demi-traverse en béton au niveau du plan de cisaillement, une fois que la partie inférieure de la boîte de cisaillement était remplie de ballast frais et compacté.
Les résultats ont été comparés aux résultats obtenus précédemment pour l'angle de frottement du ballast et pour le frottement entre gravier et béton. De plus, les résultats ont également été utilisés pour interpréter certains essais de poussée à simple lien (STPT) effectués dans l´installation d´essais ferroviaires CEDEX Track Box pour évaluer la résistance latérale de la voie.

Keywords: Ballast; sleeper; friction resistance

1 INTRODUCTION

The pass-by of trains induces vertical and horizontal loads in the railway infrastructure which must be resisted mainly by the top layer formed, in the current high speed lines, by ballast. The ballast shear strength plays an important role, especially in the case of the lateral resistance of the railway track.

There are three main components of lateral resistance, all of them associated with the interface between ballast and sleepers, and located at: the sleeper base, in the crib and in the shoulder. The contribution of each zone to the

total lateral resistance is in discussion in the literature, as shown in Table 1.

Table 1. Contribution of sleeper surfaces to total lateral resistance for unloaded track (at percentage)

Reference	Base	Crib	Shoulder
Dipilato et al. (1983)	50-60	10-20	30-40
Le Pen et al. (2011)	26-35	37-50	15-37
Kish (2011)	35-40	30-35	20-25
De Iorio et al. (2014)[(1)]	25	25	10
Estaire et al. (2017)	25-45	15-30	25-60

[(1)]Contributions to lateral strength: ballast 60%, fastening 30%, rail 10%

There are other influential factors as the train loads, the fastening system, the sleeper geometry, type and weight, type of ballast, the thickness and consolidation of ballast layer and the maintenance services [Kish (2011), De Iorio (2014)].

Therefore, given all the factors, it is evident that the friction resistance between the sleeper base and the ballast plays an essential role in the characterization of lateral resistance in railway tracks.

2 MATERIALS AND METHODS

2.1 Ballast

Ballast is a uniformly graded coarse aggregate placed between and immediately underneath the sleepers. The purpose of ballast is to provide drainage and structural support for the loading applied by trains. Aggregate type, quality, size distribution and particle shape are among the major considerations in ballasted railway track design. Usually, ballast comes from aggregates produced from crushing locally available rocks such as granite or basalt.

The normal maximum size for ballast is between 50 and 60 cm which makes it difficult to test with the usual Soil Mechanics test devices. There are a great number of published test results obtained in 30x30 cm direct shear boxes [(Dowbrow et al. (2009), Boler (2012), Wnek et al (2013), Indraratna et al. (2016)], although those boxes do not fulfill the size proportions between specimen and device stablished in the current standards (e.g. ASTM D3080). This standard sets that the ratio between specimen thickness and width is 1/2 and between maximum particle size and thickness specimen is 1/6.

To avoid this problem, derived from box size, CEDEX built, about 20 years ago, a 1x1 m direct shear box, which allows testing ballast particles without any scale effect (Estaire and Santana, 2018).

The ballast aggregates used in this study are composed of milonite and were obtained from an authorized quarry which produces railway ballast for high speed lines in Spain. Figure 1 shows the general aspect of the tested ballast.

Figure 1. General aspect of milonitic ballast used in this study

The ballast sample had particles with sizes between 25 and 60 mm, a medium diameter (D_{50}) of 40 mm and a uniformity coefficient (C_u) of 1.48. The physical properties were determined following the European Standard EN 1097-6, getting a specific weight of 2.72, a porosity of 0.54% and absorption of 0.20%. This

ballast was also characterized by EN 13450, ranking with the highest quality class.

2.2 Sleeper

The sleepers are elongated pieces located between the rails and ballast. The most common material used for its manufacturing is the wood and concrete, even, in the last years, new materials are been investigating, as recycled plastics (Belkon, 2015), or fibre-reinforced foamed urethane (FFU) (Kaewunruen et al. 2017). The sleepers main functions are: to distribute of rail loads to ballast layer; to keep rail position and level; to keep the horizontal stability of the track due to temperature or dynamic loads. The principal sleeper characteristics are: dimension, weight and elasticity. In this context, another important feature is the roughness of the sleeper bottom surface.

In Spain, the most common sleeper type used in high speed lines is the monoblock sleeper. The tests in this study were performed with the AI-04 sleeper type. It is a prestressed monoblock sleeper, with a length of 2.60 m, an outside width of 300 mm, an inner width of 227 mm, and a weight of 315 kg.

For the present study, we cut the extremes of an AI-04 sleeper for the central part to fit into the large direct shear box described below. The dimensions of the sleeper used in the tests are shown in Figure 2.

2.3 Large direct shear box

All the direct shear tests presented in this paper were performed in a very large direct shear box, belonging to the Laboratorio de Geotecnia (CEDEX) that has a shearing plane of 1 x 1 m and can hold specimens with thickness up to 80 cm, as the box height is 1.2 m. With those dimensions, and according to ASTM D3080 requirements, the maximum particle size that can be used in the tests is 8.5 cm so, in this case, all the ballast particles can be tested.

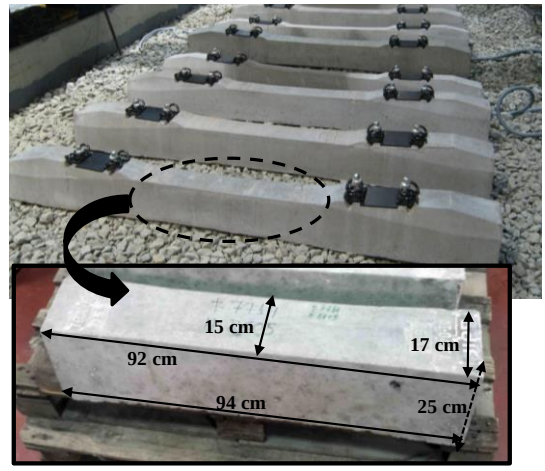

Figure 2. AI-04 EA sleeper used in the study, original and cut one.

The maximum vertical load that can be imposed to the specimen is 1000 kN. The maximum horizontal displacement of the shear test box is 25 cm, large enough to record peak shear stresses. The horizontal load, with a maximum of 1000 kN, can be imposed at a constant speed, ranging from 0.5 to 45 mm/min, although in this study a speed of 0.8 mm/min was used.

This equipment was extensively used to study rockfills for use in ports and dams. (Estaire and Olalla, 2006). In recent years, the investigations with this device have been focused on railway ballast (Estaire and Santana, 2018). Figures 3 show a photograph of the equipment used in the tests.

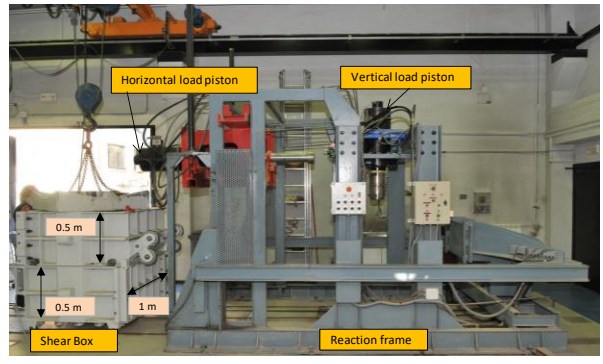

Figure 3. Photograph of the direct shear test device used in the tests

3 LARGE DIRECT SHEAR TESTS AND RESULTS

3.1 Large direct shear tests

In this study we have performed two direct shear tests in the large shear box with two different initial unit weights: in Test 1, the average unit weight of the specimens prepared for testing was 16.8 kN/m^3 while in Test 2 it was 15.6 kN/m^3. The corresponding initial void ratio (e_0) was about 0.62 and 0.75, respectively. The unit weight values obtained by this method of specimen preparation is in agreement with other values in literature: 18-14 kN/m^3 by Wnek et al. (2013), 16 kN/m^3 by Indraratna et al. (2010) or (16.1 – 17.6 kN/m^3) by Suiker et al. (2005).

The preparation begins by filling the lower part of the direct shear box with ballast, placed in three layers, each of them lightly compacted with a manual dynamic compactor, as shown in Figure 4.

After compacting the ballast layers, the part of the sleeper prepared for the tests was placed on the ballast layer surface, parallel to the shear direction, and in the shear plane (Figure 5).

Finally, after each of the tests, the sleeper was raised to check the aspect of its bottom surface (Figure 6).

Figure 4 Preparation of ballast layer with a dynamic compactor

Figure 5 Placement of the sleeper on the ballast layer at shear plane

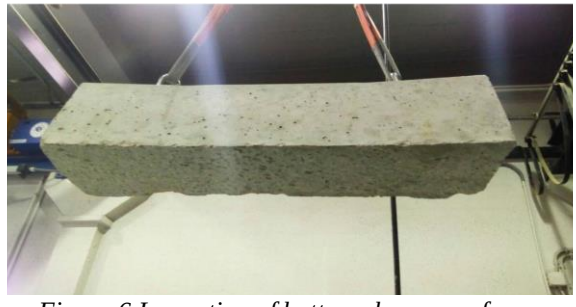

Figure 6 Inspection of bottom sleeper surface

Five different normal stresses were used in the tests: 25 kPa, 50 kPa, 100 kPa, 150 kPa and 200 kPa.

The lowest normal stresses tested (25 kPa) corresponds to the normal stress in the middle of a usual 35 cm thick ballast layer under an unloaded track. On the other hand, the intermediate low and the highest normal stresses (100 and 200 kPa) corresponds to the pressure

on the ballast layer surface transmitted by the sleeper, under a static load of a passenger train axle load (about 170 kN) and under a dynamic load of a freight train axle load (about 225 kN), respectively, acting on the horizontal sleeper area (0.65 m^2), taking into account a distribution load factor between sleepers of 0.4, due to Winkler theory (Lichtberger, 2011).

3.2 Large direct shear results for ballast-sleeper contact

Figures 7 and 8 show the results obtained in Tests 1 and 2, respectively.

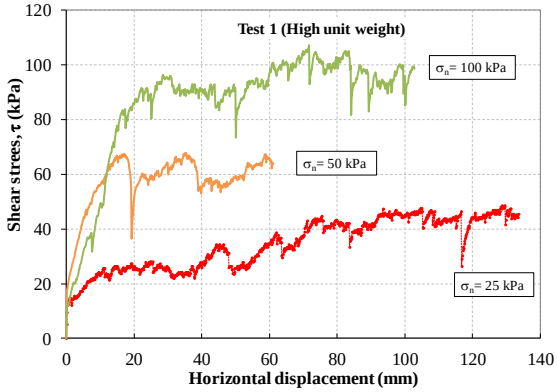

Figure 7 Shear stress-strain curves for Test 1

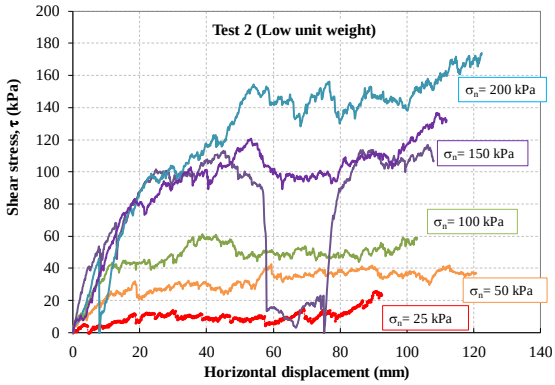

Figure 8 Shear stress-strain curves for Test 2

The horizontal displacement – shear stress curves show a slightly irregular shape and sometimes sudden shear stress drops. In all the tests, shear stress grows up continuously without reaching a clear peak, once the horizontal displacement goes up until 140 mm, the maximum allowed by this test configuration.

On other hand, Figure 9 shows the curves that relate the horizontal and vertical displacement obtained in the tests performed.

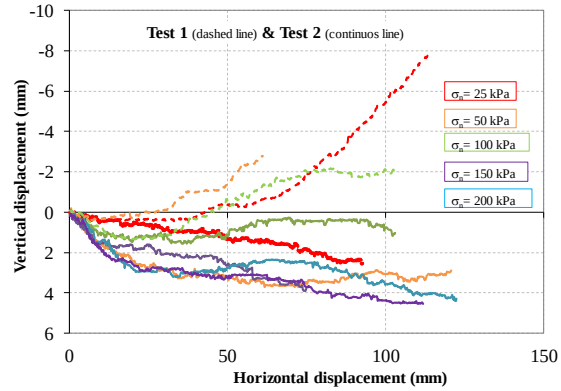

Figure 9 Horizontal v vertical displacements obtained in all the tests performed

The vertical displacement curves show a dilatant behaviour for the specimens tested in Test1, where ballast had a higher unit weight (16.8 v 15.6 kN/m^3), while for Test 2, the material shows a contractive behaviour due to its relative low unit weight.

On other hand, to have a global view of the results, Figure 10 presents the ballast-sleeper friction envelopes obtained in the tests.

Friction envelopes have been analytically expressed through two models, whose parameters are collated in Table 2:

- Mohr-Coulomb model, assuming an apparent adhesion (c*).

$$\tau = c^* + \tan \delta \, \sigma_n \qquad (1)$$

- A parabolic model, often used in ballast characterization [Indraratna et al.(1993), Jin-Cai and Chen-Xi (2016)]

$$\tau = a \, \sigma_n^{\,b} \qquad (2)$$

where a is the shear strength for σ_n=1 kPa, when τ and σ_n are expressed in kPa and b is an exponent that indicates the degree of linearity of material shear strength.

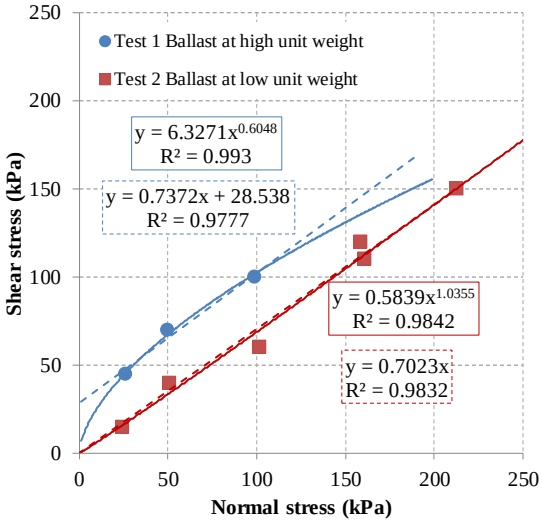

Figure 10. Ballast-sleeper friction envelopes

It can be highlighted that the regression coefficients are higher for the parabolic model, which indicates a non-linear strength behaviour in the frictional mechanism of the ballast-sleeper interface.

On other hand, the sleeper bottom surface has been checked after each test. There are not visible marks in that surface but the sleeper lateral faces have suffered little scratches. The damages in the ballast- sleeper interface can be considered as negligible.

3.3 Large direct shear results for compacted ballast specimens

As mentioned previously, we have profusely employed the large direct shear box for ballast strength characterization. At this respect, six shear stress tests obtained with compacted ballast specimens with unit weight between 15.7 and 15.9 kN/m^3, subjected to normal stresses ranging from 30 to 200 kPa, are shown in Figure 11.

It must be noted that the unit weight of the ballast specimens is very similar to the one used in Test 2.

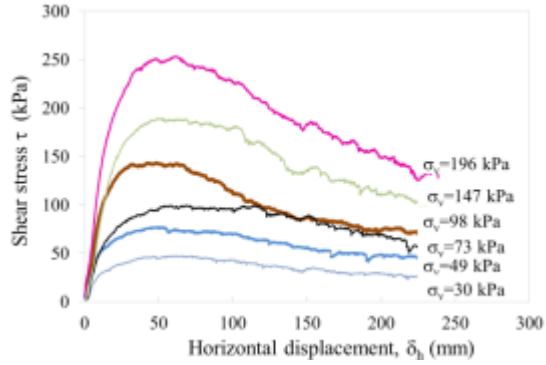

Figure 11. Shear stress curves for compacted ballast (Estaire and Santana, 2018).

It can be seen that the curves obtained with the ballast compacted specimens are quite different from curves in Figures 7 and 8. They are quite smooth and show very marked peak strengths.

Figure 12 presents the ballast failure envelope with the same models described previously. The parameters obtained from the tests are also shown in Table 2.

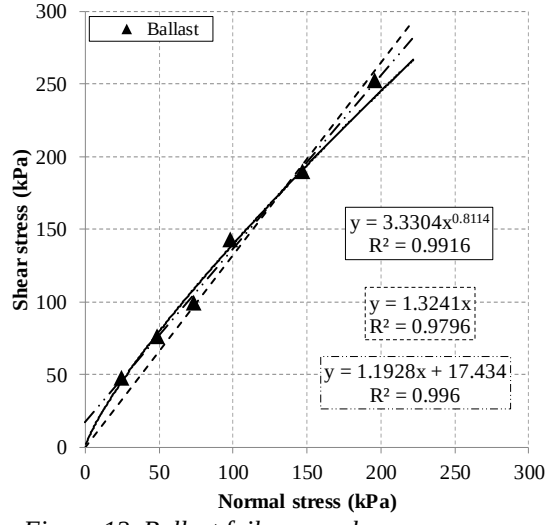

Figure 12. Ballast failure envelope

4 RESULT DISCUSSION

This section deals with the comparison between the results obtained in the direct shear tests

performed with ballast and in the ballast-sleeper interface.

4.1 Failure envelope

The first way of comparison is through the failure and friction envelopes, as shown in Figure 13 and Table 2.

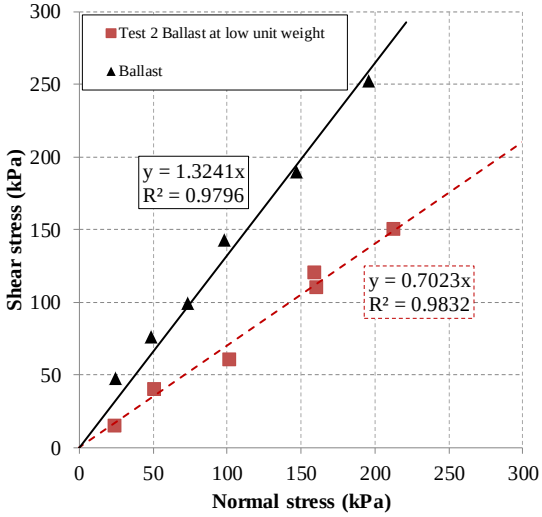

Figure 13. Comparison between ballast failure and ballast-sleeper friction envelopes

Table 2. Parameters of the models to interpret ballast-sleeper friction

Test	Unit weight kN/m³	Mohr-Coulomb model c*//c (kPa)	Mohr-Coulomb model δ // ϕ (º)	Parabolic model a	Parabolic model b
T1	16.8	28	36	6.33	0.61
T2	15.6	0	35	0.58	1.04
Ballast	15.7-15.9	0-17	53-50	3.33	0.81

The most important output from these tests is the comparison between the friction angles obtained in the tests with ballast (ϕ=53º) and in the ballast-sleeper interface (δ=35º) of Test 2, both of them performed with very similar unit weight. It can be noted that, according to the results, $\delta=2/3\phi$º, which is a very usual value used in many geotechnical engineering applications when there is an interface between concrete and soil.

On other hand, when comparing Tests 1 and 2, it seems that the increase in unit weight produces an increase in adhesion (from 0 to 28 kPa) in the interface, while the friction angle maintains its value (around 35º). The parabolic model parameters are quite different.

4.2 Shear stresses

Another way of analysing the results is the comparison between shear stresses obtained for different normal stresses, as shown in Table 3

Table 3. Comparison between shear stresses obtained in the tests

	Normal stress (kPa)				
	25	50	100	150	200
Test	Shear stress (kPa)				
T1	45	70	100	---	---
T2	15	40	60	120	150
Ballast	47	76	143	189	252
	Ratio				
T2/T1	0.33	0.57	0.60	---	---
T2/B	0.32	0.53	0.42	0.63	0.60

When comparing Test 1 and 2, the increase in unit weight (15.6 v 16.8 kN/m^3) makes shear stress be between 0,35 and 0,60 compared to the values obtained in Test 1.

However, when the comparison is made between the tests performed with ballast prepared with the similar unit weight, shear stress in the sleeper-ballast interface are between 0.32 and 0.63 of the value obtained in the ballast specimens, with an average value of 0.50.

5 SUMMARY AND CONCLUSSIONS

Two direct shear tests were performed in a large shear box (1x1 m) to determine the friction in the interface between ballast and the sleeper bottom surface. These results were compared

with previously performed direct shear tests with compacted ballast.

The main conclusions that can be drawn are:

- The friction angle in the sleeper-ballast interface (δ) can be determined, according to the results obtained, as $\delta=2/3\phi$, being ϕ the ballast friction angle.
- This result ($\delta=2/3\phi$) should be used in the analysis of the different lateral resistance tests to determine the contributions of the different sleeper zones in such resistance.
- Shear stress in the sleeper-ballast interface are as an average 0.50 of those obtained in ballast.

6 ACKNOWLEDGEMENTS

The authors of the paper wish to acknowledge the people who performed the tests (Jose L. Gómez, Oscar Tello, Rafael Rodríguez and Mauro Muñiz) for their dedication and effort.

7 REFERENCES

Belkon, A. 2015. Recycled plastic railway sleepers. Analysis and comparison of sleeper parameters and the influence on track stiffness and performance. *Railway Engineering. 13 th Int. Conf. and Exhibition.* Edinburgh, UK, 30th June/1st July.

Boler, H. 2012. On the shear strength of polyurethane coated railroad ballast. *PhD Thesis, Univ. Illinois at Urbana Champaign*.

De Iorio, A., Grasso, M., Penta, F., Pucillo, G. and Rosiello, V. 2014. Transverse strength of railway tracks: part 2. Test system for ballast resistance in line measurement. *Frattura ed Integrità Strutturale*, 30, 578-592.

Di Pilato, M. A., Levergood, A. V., Steinberg, E. I. and Simon, R. M. 1983. Railroad track substructure design and performance evaluation practice. *Goldberg-Zoino and Ass. Inc., Newton Upper Falls, Massachusetts, Report No. FRA/ORD83/04.2*, June, 65.

Dowbrow, W., Huang, H. and Tutumluer. E. 2009. Comparison of coal dust fouled railroad ballast behavior – granite vs. limestone. *Proceedings of 8th International Conference on Bearing Capacity of Roads and Airfields*, Volume 2, 1349-1360.

Estaire, J. and Olalla, C. 2006. Analysis of strength of rockfills based on direct shear tests made in 1 m^3 box. *22nd International Congress ICOLD*. Q.86-R.36. , 529-540.

Estaire, J. and Santana, M. 2018. Large direct shear tests performed with fresh ballast. *Railroad Ballast Testing and Properties, ASTM STP1605*. T.D. Stark, R. Szecsy and R.H. Swan, Jr., Eds., ASTM Int., New Orleans.

Estaire, J., Cuéllar, V. and Santana, M. 2017. Track lateral stability tests performed in CEDEX Track Box and their modelling. *Geotecnia* 140 *julio, 03-30*. http://dx.doi.org/10.24849/j.geot.2017.140.01

Indraratna, B., Nimbalkar, S.S. and Ngo, N.T. 2016. Performance improvement of rail track substructure using artificial inclusions. Experimental and numerical studies. *Transp Geotec.* 8: 69-85.

Indraratna, B., Nimbalkar, S.S., Tennakoon, N. 2010. Behaviour of ballasted track foundations: Track drainage and geosynthetic reinforcement. *GeoFlorida 2010: Advances in Analysis, Modelling & Design*. Orlando.

Indraratna, B., Wijewardena, L., Balasubramaniam, A. 1993. Large-scale triaxial testing of greywacke rockfill. *Geotechnique,* 43 *(1), 37-51.*

Jin-Cai, Z. and Chen-Xi, T. 2016. Shear strength of railway ballast. *EJGE,* 21, Bund. 16, 4759-4771.

Kaewunruen, S., You, R. and Ishida, M. 2017. Composites for timber-replacement bearers in railway S&C. *Infrastructures 2 ,13*.

Kish, A. 2011. On the fundamentals of track lateral resistance. AREMA Annual conference, September 18-21.

Le Pen, L. and Powrie, W. 2011. Contribution of base, crib and shoulder ballast to the lateral sliding resistance of railway track: a geotechnical perspective. *J. Rail and Rapid Transit*, 225,113

Lichtberger B. Manual de vía. (2011) Eurail Press. ISBN 978-3-7771-0409-6.

Suiker, A., Seling, E., Frenkel, R. 2005. Static and cyclic triaxial testing of ballast and subballast. *J. Geotech. and Geoenvironmental Eng.*, Vol. 131, No. 6, 771-782.

Wnek, M.A., Tutumluer, E., Moaveni, M. 2013. Investigation of Aggregate Properties Influencing Railroad Ballast Performance, *Journal of the Transportation Research Board,* 2374, 180-189.